

Spectroscopic Properties of the CP43 Core Antenna Protein of Photosystem II

Marie-Louise Groot, Raoul N. Frese, Frank L. de Weerd, Krystyna Bromek, Åsa Pettersson, Erwin J. G. Peterman, Ivo H. M. van Stokkum, Rienk van Grondelle, and Jan P. Dekker

Division of Physics and Astronomy, Institute of Molecular Biological Sciences, Vrije Universiteit, 1081 HV Amsterdam, the Netherlands

ABSTRACT CP43 is a chlorophyll-protein complex that funnels excitation energy from the main light-harvesting system of photosystem II to the photochemical reaction center. We purified CP43 from spinach photosystem II membranes in the presence of the nonionic detergent *n*-dodecyl- β , β -maltoside and recorded its spectroscopic properties at various temperatures between 4 and 293 K by a number of polarized absorption and fluorescence techniques, fluorescence line narrowing, and Stark spectroscopy. The results indicate two “red” states in the Q_y absorption region of the chlorophylls. The first peaks at 682.5 nm at 4 K, has an extremely narrow bandwidth with a full width at half-maximum of ~ 2.7 nm (58 cm $^{-1}$) at 4 K, and has the oscillator strength of a single chlorophyll. The second peaks at ~ 679 nm, has a much broader bandshape, is caused by several excitonically interacting chlorophylls, and is responsible for all 4 K absorption at wavelengths longer than 685 nm. The Stark spectrum of CP43 resembles the first derivative of the absorption spectrum and has an exceptionally small overall size, which we attribute to opposing orientations of the monomer dipole moments of the excitonically coupled pigments.

INTRODUCTION

Photosystem II (PSII) is a large supramolecular pigment-protein complex embedded in the thylakoid membranes of green plants, algae, and cyanobacteria. The green plant PSII consists of at least 25 different types of protein subunits, many of which are bound to the thylakoid membranes (Hankamer et al., 1997). Some subunits have a light-harvesting or antenna function, i.e., they are involved in the capturing of solar energy, the efficient transfer of the excitation energy to the photochemical reaction center, and the regulation of the energy flow. There are two groups of light-harvesting complexes in PSII. The first is formed by the core antenna proteins CP47 and CP43. These chloroplast-encoded, sequence-related proteins each bind ~ 14 chlorophyll *a* (Chl *a*) and two or three β -carotene (β -Car) molecules (Hankamer et al., 1997) and are closely associated with the photochemical reaction center (Eijkelhoff et al., 1997; Hasler et al., 1997; Rhee et al., 1998). The second group is formed by the peripheral antenna, which in green plants consists of a collection of nuclear-encoded sequence-related Chl *a/b* binding proteins. This group of proteins is generally referred to as light-harvesting complex II (LHCII) and does not show sequence homology with the core antenna proteins.

The largest isolated and purified PSII particles are the so-called PSII-LHCII supercomplexes and megacomplexes, and several tens of such associations have now been characterized by electron microscopy and single-particle image averaging techniques (Boekema et al., 1995, 1998, 1999). They all consist of one or two dimeric PSII core complexes, which are surrounded by a variable number of peripheral trimeric and monomeric LHCII proteins. These structures show how the various PSII proteins are connected and, in particular, what the pathways of excitation energy transfer might be from the peripheral antenna to the photochemical reaction center. For instance, it now seems clear that in all supercomplexes the CP43 antenna protein (the subject of this paper) funnels the excitation energy from the minor Chl *a/b* antenna protein CP26 to the reaction center, while in some larger associations it may accept excitation energy from trimeric LHCII as well (Boekema et al., 1999).

Considerably more structural detail has been obtained by electron crystallography of two-dimensional crystals of the CP47-RC complex (Rhee et al., 1997, 1998). The structure reveals 23 transmembrane α -helices, of which 10 can be assigned to the D1D2 reaction center complex and six to CP47. Preliminary locations of 14 Chl molecules in CP47 and four Chl and two pheophytin molecules in the RC were also suggested. These data provided, for the first time, some understanding of the structural organization of a PSII core antenna protein, and in addition suggested a structural similarity between the core antenna parts of PSII and PSI (see also Schubert et al., 1998). The general motif seems to be that the core antenna proteins consist of three pairs of transmembrane α -helices that bind ~ 14 chlorophylls in two layers near the upper and lower parts of the membrane (Rhee et al., 1998).

Despite their important roles in the overall function of PSII, the spectroscopy of the core antenna complexes has not been characterized in very much detail. Important rea-

Received for publication 24 June 1999 and in final form 30 August 1999.

Address reprint requests to Dr. Jan P. Dekker, Division of Physics and Astronomy, Institute of Molecular Biological Sciences, Vrije Universiteit, De Boelelaan 1081, 1081 HV Amsterdam, the Netherlands. Tel.: 31-20-444-7931; Fax: 31-20-444-7999; E-mail: dekker@nat.vu.nl.

Dr. Groot's present address is INSERM U451, Laboratoire d'Optique Appliquée, Ecole Polytechnique ENSTA, 91761 Palaiseau Cedex, France.

Dr. Peterman's present address is Department of Chemistry and Biochemistry, University of California, San Diego, 9500 Gilman Drive, La Jolla, CA 92093-0340.

sons for this lack of knowledge are perhaps the difficulty by which the complexes can be isolated and purified and the instability of the purified complexes. The CP47 protein has been spectroscopically analyzed by a few groups (see, e.g., Groot et al., 1995, and references therein), but a CP43 complex with distinct spectroscopic features has only been prepared from a thermophilic cyanobacterium (Breton and Katoh, 1987). Nevertheless, a good understanding of the spectroscopy is required to understand the role of these proteins in the energy migration to the reaction center.

Some time ago, we presented a new method to isolate and purify the CP43 complex from spinach, and we presented a preliminary spectroscopic characterization (Dekker et al., 1995). In this report, we present a much more detailed spectroscopic characterization of the purified material by polarized, site-selective absorbance-difference spectroscopy, fluorescence line narrowing (FLN), circular dichroism (CD), linear dichroism (LD), and Stark spectroscopy. Our results show that the spectroscopic properties of CP43 are dominated by excitonic coupling between (sub-)groups of pigments, and that the complex has two different low-energy states at low temperatures with different peak positions and bandwidths, one of which gives rise to the narrowest chlorophyll absorption band observed in chlorophyll-containing complexes thus far.

MATERIALS AND METHODS

The first step of the isolation and purification of the CP43 complex involved the preparation of PSII core complexes from spinach as described by Ghanotakis et al. (1987). These preparations were Tris-washed, solubilized with *n*-dodecyl- β , β -maltoside (β -DM), and subjected to ion-exchange chromatography as described by Dekker et al. (1989), except that MgSO_4 was omitted from the buffers. Under these conditions, the CP47-RC complex and the 28-kDa protein were bound by the Q-Sepharose column, whereas CP43 was found in the fraction that did not bind to the column. This fraction was dialyzed overnight against 50 mM Tris-HCl (pH 7.8) + 0.03% β -DM, after which it was applied to a Q-Sepharose column (Pharmacia) equilibrated with 50 mM Tris-HCl (pH 7.8) + 0.03% β -DM. After the eluate (which contained mainly free Chl) became colorless, CP43 was eluted with the same buffer + 50 mM MgSO_4 . Its purity was checked by fast protein liquid gel filtration chromatography (Eijkelhoff et al., 1996), and in case of impurities the fraction was recycled through the anion-exchange column as described above. The sample was diluted in a buffer containing 20 mM BisTris (pH 6.5), 20 mM NaCl, 0.03% β -DM, and 75% (v/v) glycerol, to an optical density (OD) as described in the figure legends. Samples for Stark measurements were concentrated on the same ion-exchange column to an OD of $\sim 60 \text{ cm}^{-1}$, after which they were diluted in a buffer described above, but with 0.05% (w/v) β -DM and 92% glycerol (v/v). The low-temperature measurements were performed in an Oxford liquid nitrogen bath cryostat or in a Utreks liquid helium flow cryostat.

Absorption spectra were recorded with a Cary 219 spectrophotometer with 0.5-nm resolution. Nonselectively excited emission spectra were recorded as described by Groot et al. (1994), using broad-band (12 nm full width at half-maximum (fwhm)) 610-nm light as the excitation source. Site-selective absorbance difference spectra were measured as described by Kwa et al. (1994a), while site-selective emission spectra were recorded as described by Peterman et al. (1997, 1998a). Briefly, a CW dye laser (Coherent CR599) with DCM dye and a bandwidth of $\sim 0.1 \text{ nm}$, pumped by an Ar^+ laser (Coherent Innova 310), was used for excitation. The power was attenuated to $50 \mu\text{W}/\text{cm}^2$, and an illumination time of no more than

40 s was used for the emission measurements, to avoid hole burning. For the absorbance-difference spectra a power of $18 \text{ mW}/\text{cm}^2$ was used to create a significant steady-state population of the triplet state. The absorbance-difference spectra were measured with double lock-in detection and a monochromator with 3-nm resolution. Emission spectra were detected with a 0.5-m spectrograph (Chromex 500IS) and a CCD camera (Chromex Chromcam 1) with 0.25- or 0.5-nm resolution. Parallel and perpendicular polarized spectra were measured by rotating a polarizer behind the sample relative to a polarizer in front of the sample (Kwa et al., 1994a).

Circular dichroism was recorded on a home-built apparatus as done by Visschers et al. (1991). For the linear dichroism (LD) experiment a mild gel based on gelatin was used (see, e.g., Otte et al., 1992), containing 20 mM HEPES (pH 7.9), 20 mM NaCl, 0.09% β -DM, 75% (v/v) glycerol, and 6.4% (w/v) gelatin. The sample was diluted in the molten gel (at $\sim 32^\circ\text{C}$) to an optical density of 0.6 cm^{-1} (675 nm, 77 K). The absorption spectrum was recorded simultaneously to check that the absorption spectrum was not affected by the gel and the elevated temperature. The $12.5 \times 12.5 \text{ mm}$ polymerized gel was oriented by squeezing in two perpendicular directions to the $10 \times 10 \text{ mm}$ dimensions of the cuvette.

Stark spectroscopy was performed as done by Beekman et al. (1997b). For randomly oriented and fixed molecules the Stark lineshape is usually described by a sum of the zeroth, first, and second derivatives of the ground-state absorption spectrum, which give information on field-dependent changes of the oscillator strength of the optical transition, the difference polarizability between the excited state and ground state of the molecule ($\text{Tr}\Delta\alpha$), and the difference in permanent dipole moment between the excited state and ground state of the molecule ($\Delta\mu$), respectively (Liptay, 1974; Boxer, 1996; Somsen et al., 1998). Furthermore, the dependence of the signal on the angle χ between the applied electric field and the polarization direction of the light gives information on the orientation of $\Delta\mu$ and $\Delta\alpha$ with respect to the transition dipole.

Stark and absorption spectra were simultaneously fitted using a nonlinear least-squares fitting program (Beekman et al., 1997a,b) with (skewed) Gaussian functions for the absorption spectrum and zeroth, first, and second derivatives of this function for the Stark spectrum, thus providing estimates of $\Delta\mu$ and $\text{Tr}\Delta\alpha$ for each Gaussian function.

RESULTS AND DISCUSSION

Absorption

Fig. 1 shows the 5 K absorption spectrum of the purified CP43 complex. The peak at 437 nm is caused by the Soret band of chlorophyll *a*, while the peaks at 497 and 462 nm can be assigned to β -carotene. The peak positions of the β -carotenes are slightly blue-shifted compared to those of

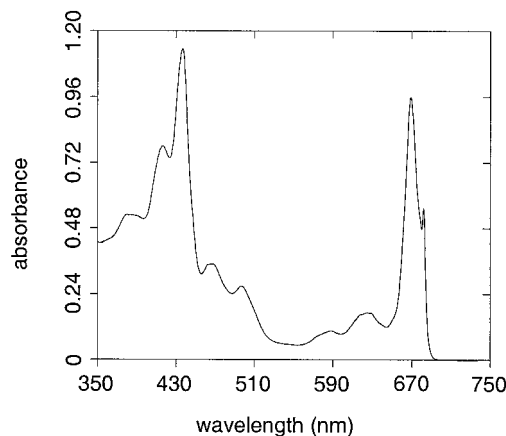


FIGURE 1 Absorption spectrum at 5 K of the purified CP43 complex.

CP47, which occur at 502 and 467 nm at 4 K (Groot et al., 1995). This difference in peak position vanishes as the temperature is increased to $T = 293$ K. At this temperature the red-most band peaks at ~ 494 nm in both CP43 (not shown) and CP47 (Renge et al., 1996). Both core antenna complexes, however, do not show the unusual β -carotene absorption of the photosystem II reaction center complex (Van Dorssen et al., 1987a), which has been interpreted as the result of excitonic coupling between two β -carotene molecules (Newell et al., 1991; Renge et al., 1996).

Fig. 2 A (*solid line*) shows an enlargement of the chlorophyll Q_y absorption region of CP43 together with its second derivative (*dash-dotted line*). The absorption spectrum shows a broad maximum at 669 nm and a very distinct and narrow peak at 682 nm. The second derivative shows maxima at 682.5, 678, 668.5, and 660.5 nm and a shoulder near 672 nm, which suggests that this part of the absorption spectrum is caused by at least four different spectral components. Also shown is the emission spectrum at 5 K (*dashed line*), from which it becomes immediately clear that the Stokes' shift of the complex is very small. Fig. 2 B shows the temperature dependence of the Q_y absorption between 5 K and 293 K. The spectrum broadens considerably as the temperature is increased, and the sharp 682-nm band vanishes as the temperature is increased above 77 K.

Our absorption spectra are roughly similar to the 48 K spectrum reported by Alfonso et al. (1994) and the 8 K spectrum reported by Carbonera et al. (1992), although in these spectra the 682-nm feature appears only as a shoulder. The 10 K spectrum of CP43 of the thermophilic cyanobacterium *Synechococcus elongatus* (Breton and Katoh, 1987) is even more similar, because this spectrum also reveals a narrow peak at 682 nm. We note that the 4 K spectrum of a well-resolved PSII core preparation from spinach also reveals a narrow peak at 682 nm (Van Leeuwen, 1993). This feature is most likely caused by CP43, because the other constituents in the PSII core do not exhibit a separate peak at 682 nm (see, e.g., Groot et al., 1995; Eijkelhoff et al., 1996) and because the CP47-RC and CP43 spectra have been shown to add up to the PSII core spectrum (Breton and Katoh, 1987).

Fig. 2 C shows a fit of the 5 K absorption spectrum with Gaussian bands. We note that this fit should be interpreted with much care, because a unique fit is seldom found and because there is no good evidence that absorption bands at 5 K have Gaussian shapes. The result shown in Fig. 2 C is a fit with five bands, of which all parameters (peak position, bandwidth, and intensity) have been used as free fit parameters. The final result differed slightly when different starting conditions were used. In all fits, however, the red-most part of the absorption is described by a very narrow band (fwhm ≈ 2.7 nm, or 58 cm^{-1}) peaking at 682.5 nm and a much broader band peaking at slightly shorter wavelength (*bands 1 and 2, respectively, in Fig. 2 C*). The integrated intensity of band 1 is rather small ($\sim 5\%$ of the intensity of bands 1–5 of the fit shown in Fig. 2 C), suggesting that band 1 does not carry more intensity than that of a single chlo-

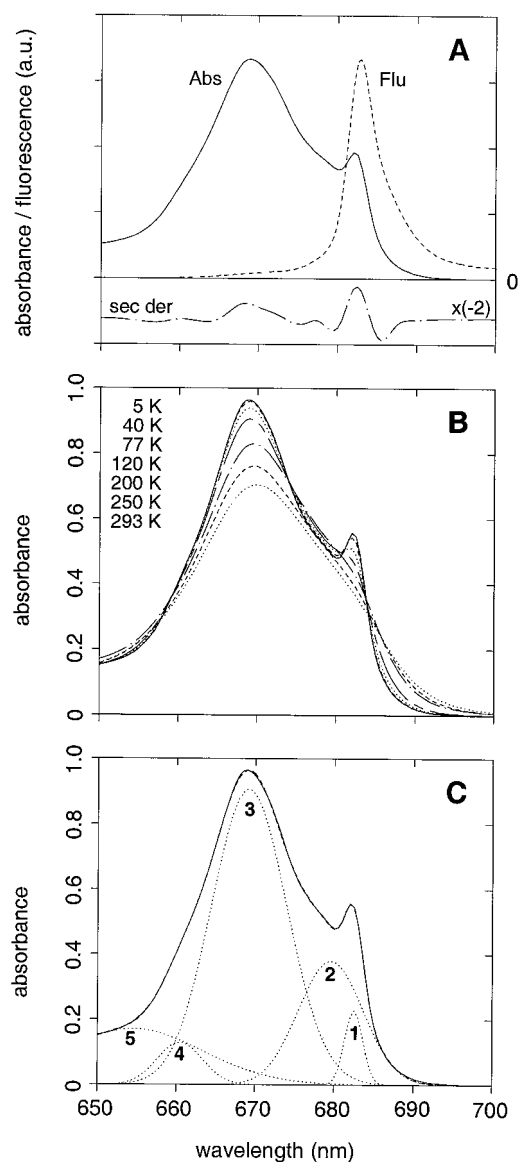


FIGURE 2 (A) Absorption spectrum at 5 K of CP43 in the Q_y absorption region of the chlorophylls (*solid line*). Also shown are the second derivative of the 5 K absorption spectrum (*dash-dotted line*, multiplied by -2) and the nonselectively (615 nm) excited 5 K emission spectrum of CP43 (*dashed line*). (B) The red part of the absorption spectrum of CP43 at $T = 5, 40, 77, 120, 200, 250,$ and 293 K (from top to bottom at 669 nm, respectively). (C) Comparison of the 5 K absorption spectrum (*solid line*) with a fit with five Gaussian bands (*dashed line*) as described in the text. *Dotted lines*: The five spectral components used for this fit (see Table 1 for details).

rophyll. At higher temperatures, the bandwidth of band 1 increases considerably (at 77 K its bandwidth is ~ 3.3 nm), but its intensity remains small in the fits. Table 1 summarizes the outcomes of the various fits.

We note that a very different fit of the 5 K absorption spectrum can be obtained if the assumption of a Gaussian lineshape is omitted. For instance, the sharp peak at 682 nm and a part of the red tail of the spectrum can also be explained perhaps by assuming a Lorentzian lineshape of

TABLE 1 Results of the fitting of the CP43 absorption (Abs) and fluorescence (Fluor) spectra at three temperatures with five (Abs) and four (Fluor) Gaussian bands

Temperature	Band 1	Band 2	Band 3	Band 4	Band 5
Abs	682.5 nm	679.6 nm	669.2 nm	660.5 nm	654.5 nm
4 K	2.7 nm	9.5 nm	11.3 nm	6.8 nm	20.7 nm
	0.23	0.38	0.91	0.13	0.17
Abs	682.5 nm	679.1 nm	668.9 nm	660.3 nm	654.8 nm
77 K	3.3 nm	10.6 nm	11.0 nm	7.0 nm	21.1 nm
	0.16	0.41	0.85	0.13	0.17
Abs	682.5 nm	679.1 nm	668.9 nm	660.3 nm	654.1 nm
200 K	5.1 nm	13.4 nm	11.7 nm	9.0 nm	23.4 nm
	0.05	0.41	0.67	0.11	0.17
Fluor	682.7 nm	684.5 nm	678.7 nm		692.8 nm
4 K	3.0 nm	7.5 nm	17.3 nm		13.9 nm
	0.597	0.414	0.047		0.078
Fluor	682.9 nm	683.6 nm	682.7 nm		702.0 nm
80 K	3.4 nm	8.2 nm	18.0 nm		22.6 nm
	0.319	0.439	0.244		0.050
Fluor	683.8 nm	681.9 nm	670.8 nm		699.8 nm
200 K	6.0 nm	15.1 nm	10.4 nm		18.7 nm
	0.188	0.813	0.215		0.107

The data indicate the peak wavelength, bandwidth (full width at half-maximum), and intensity, respectively, and correspond to the spectra shown in Fig. 2 C (Abs) and Fig. 3 B (Fluor). All parameters were used as free fit parameters, except for the peak wavelengths of band 1 in the 77 K and 200 K absorption spectra, which were fixed at 682.5 nm.

the 682-nm transition. We will show in the following, however, that several spectroscopic features can only be explained by two different red transitions, and in particular the fluorescence line-narrowing data described below provide clear evidence for the existence of two red bands with very similar lineshapes and peak wavelengths as depicted in Table 1. These results suggest that the 5 K absorption spectrum of CP43 can be explained reasonably well by a set of Gaussian bands.

Emission

Fig. 3 A shows emission spectra between 5 K and 260 K recorded upon nonselective excitation at 615 nm. The spectrum at 5 K (*continuous line*) peaks at 682.8 nm and has a fwhm of 4.5 nm. The spectrum is clearly asymmetrical, showing an intense tail on the long-wavelength side between 685 and 688 nm. The emission at ~ 670 nm is probably due to unconnected chlorophyll *a* (see Kwa et al., 1994; Groot et al., 1995). The amount of unconnected chlorophyll must be very small because the integrated emission at 670–675 nm is not more than a few percent (Fig. 3 A), and the fluorescence quantum yield of unconnected chlorophyll is probably higher than that of CP43 (see below).

As the temperature is increased from 5 K to 260 K, there is an increase of short-wavelength emission, which results in a broadening from 4.7 nm at 5 K, via 6.4 nm at 80 K, to 20 nm at 260 K. The quantum yield of the fluorescence, obtained by integrating the total fluorescence and calibrated with free Chl *a* as described by Groot et al. (1994), is $\sim 10\%$ at 4 K and gradually decreases with temperature to 50% of its low temperature value at 260 K (not shown). A similar

temperature dependence of the fluorescence yield was observed for CP47, which was explained by a promoting/accepting mode in the internal conversion process on the order of 350 cm^{-1} (Groot et al., 1995).

Fig. 3 B presents a fit of the 5 K emission spectrum with Gaussian bands (see also Table 1). Also in this case the outcome has to be interpreted with caution. Nevertheless, it is striking to see that the main part of the emission is composed of two Gaussian bands that correspond rather well to bands 1 and 2 of the 5 K absorption spectrum. Also here a very narrow band occurs, which is designated again as band 1 and which is only very slightly broader and red-shifted compared to the corresponding band in the absorption spectrum. Band 2 is broader but considerably red-shifted and narrower in emission than in absorption, which can be explained by downhill energy transfer within this band and/or to band 1. Only the red part of the inhomogeneous distribution of this component will therefore give rise to long-lived fluorescence.

The narrow width and asymmetry of the emission are in striking contrast with the CP47 emission spectrum at 4 K, which shows a symmetrical band and has a width of 12.5 nm fwhm (Groot et al., 1995). A relatively narrow 4 K emission spectrum has been recorded, however, for the trimeric LHCII complex (Kwa et al., 1992), which reveals a width of 5.5 nm (fwhm). Band 1 in CP43, however, is even narrower and is probably the narrowest absorption band observed thus far in any chlorophyll-protein complex.

Fluorescence line narrowing

A technique for obtaining high-resolution emission spectra is fluorescence line narrowing (Personov, 1983). In this

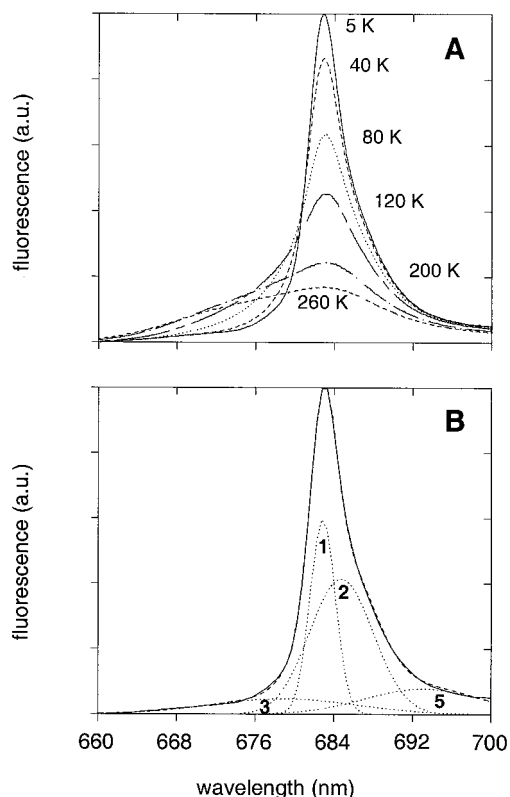


FIGURE 3 (A) Emission spectra of CP43 at $T = 5, 40, 80, 120, 200,$ and 260 K, excited at 615 nm with the same number of incident photons. (B) Comparison of the 5 K emission spectrum (solid line) with a fit with four Gaussian bands (dashed line) as described in the text. Dotted lines: The four spectral components used for this fit (see Table 1 for details). The numbers correspond to the spectral components observed in the absorption spectrum.

technique emission spectra are recorded with sub-nm resolution upon narrow-bandwidth ($\sim\text{cm}^{-1}$) continuous-wave laser excitation. When energy transfer reactions can be

avoided by exciting the sample at low temperature in the red edge of the absorption spectrum, a narrow distribution of sites is excited, leading to fluorescence line narrowing (FLN). FLN spectra have recently been reported for the chlorophyll(s) of the trimeric light-harvesting complex (LHCII) from spinach (Peterman et al., 1997), the photosystem II reaction center complex from spinach (Peterman et al., 1998a), and the cytochrome b_6f complex from *Synechocystis* PCC 6803 (Peterman et al., 1998b).

Fig. 4 shows the 5 K emission spectrum of CP43 obtained upon excitation in the far red edge of the absorption spectrum (the emission spectra recorded with $\lambda_{\text{exc}} = 685.5, 686.3,$ and 687.2 nm, each converted to the wavenumber scale, plotted as the difference with the excitation wavenumber and summed). The peak at 0 cm^{-1} is not only caused by scattered excitation light, but to some extent also by the purely electronic emission from the zero-phonon line (ZPL). The sharp peaks up to $\sim 1700\text{ cm}^{-1}$ arise from a large number of vibrational zero-phonon lines (vZPL), while the broader wing with features at $24, 52,$ and 86 cm^{-1} (Fig. 4, inset) represents the phonon wing (PW). The PW is probably caused by rearrangements of (part of) the protein backbone, while the vZPLs can be viewed as less intense repeats of the complete ZPL/PW structure, separated by frequencies of vibrational modes.

The peak position of the PW (24 cm^{-1}) occurs at about the same wavenumber as the PW observed in LHCII (Peterman et al., 1997) and cytochrome b_6f (Peterman et al., 1998b). In contrast to the latter systems, however, a 52 cm^{-1} mode can be distinguished, which most likely can be attributed to the first overtone of the 24 cm^{-1} mode. In the PSII RC both modes occur at lower wavenumber (Peterman et al., 1998a). The 86 cm^{-1} mode may be the second overtone, but it may also be an extra low-frequency mode caused by an intermolecular vibration of excitonically coupled chlorophylls, as discussed recently for the PSII RC

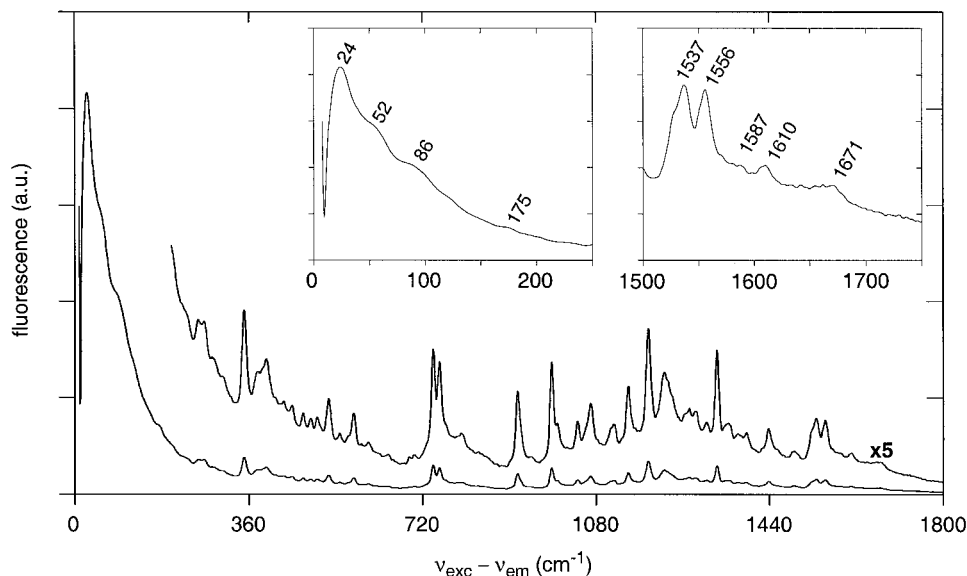


FIGURE 4 Line-narrowed emission spectra of CP43 at 5 K. The spectra are the average of the spectra excited at $685.5, 686.3,$ and 687.2 nm, each converted to the wavenumber scale and plotted as the difference with the excitation wavenumber. The upper spectrum is a $5\times$ magnification to enhance details in the vibronic region. Insets: Magnifications of the PW region (left) and the region of the chlorin C=C and 13^1 C=O stretch modes (right).

(Peterman et al., 1998a). The frequencies of the chlorin C=C stretch modes at 1537, 1556, and 1610 cm^{-1} (Fig. 4, *inset*) indicate one axial protein ligand of the central magnesium, although the shoulder at 1527 cm^{-1} may suggest the presence of an additional contribution of chlorophyll with two axial protein ligands. In the case of two axial ligands these modes are known to occur at a $\sim 10 \text{ cm}^{-1}$ lower wavenumber (Fujiwara and Tasumi, 1986a,b). The weak band at 1671 cm^{-1} (Fig. 4, *inset*) probably reflects the $^{13}\text{C}=\text{O}$ stretch mode of Chl *a* (Lutz and Robert, 1988), and its particular frequency suggests hydrogen bonding to the protein environment. Without hydrogen bonding this transition is expected to shift to $\sim 1690 \text{ cm}^{-1}$ (Lutz and Robert, 1988).

Fig. 5, A and B, shows the excitation wavelength dependence of two parts of the vibrational finestructure. The excitation wavelength of 680.3 nm hardly induces any fine structure in the emission, which suggests that excitation at this wavelength mainly results in downhill energy transfer to other pigments, thus abolishing the line narrowing. With excitation at wavelengths between 682 and 687 nm, however, downhill energy transfer does not seem to be possible at 4 K, and considerable line-narrowing occurs (see, e.g., the modes at 349 and 1330 cm^{-1}). The line-narrowing pattern shows considerable variation when the excitation wavelength is scanned (Fig. 5, A and B). There are several bands that are easily recognizable upon excitation between 682.1 and 684.7 nm but virtually absent upon excitation above 685.5 nm (e.g., bands at 415, 544, 561, and 1231 cm^{-1}). The most straightforward explanation for this behavior is that excitation between 682.1 and 684.7 nm gives rise to emission from two different pools of chlorophylls, whereas excitation above 685.5 nm induces emission from a single pool of chlorophylls. This interpretation is in excellent agreement with the results from the fitting with Gaussian bands (Fig. 2 C). Below 685 nm two different spectral forms (bands 1 and 2) contribute to the absorption spectrum, whereas above 685 nm only band 2 contributes. The contribution of band 1 in the mixed spectrum also gives rise to a new band at 1658 cm^{-1} and a much smaller amplitude of the shoulder at 1527 cm^{-1} (Fig. 5 C), suggesting that indeed a different pool of chlorophylls is excited with a stronger hydrogen bonding of the $^{13}\text{C}=\text{O}$ group and a smaller contribution from chlorophylls with two axial protein ligands. We note that the finding of two different emitters in CP43 is rather unique. FLN experiments on the PSII RC (E. J. G. Peterman, unpublished observations) and CP47 (F. L. de Weerd, unpublished observations) have indicated that in these systems only one pool of chlorophyll with one type of vibrational fine structure causes the 4 K fluorescence.

Triplet-minus-singlet absorbance difference spectroscopy

The excited state of Chl *a* does not only decay to the ground state (either radiatively, as discussed above, or via internal

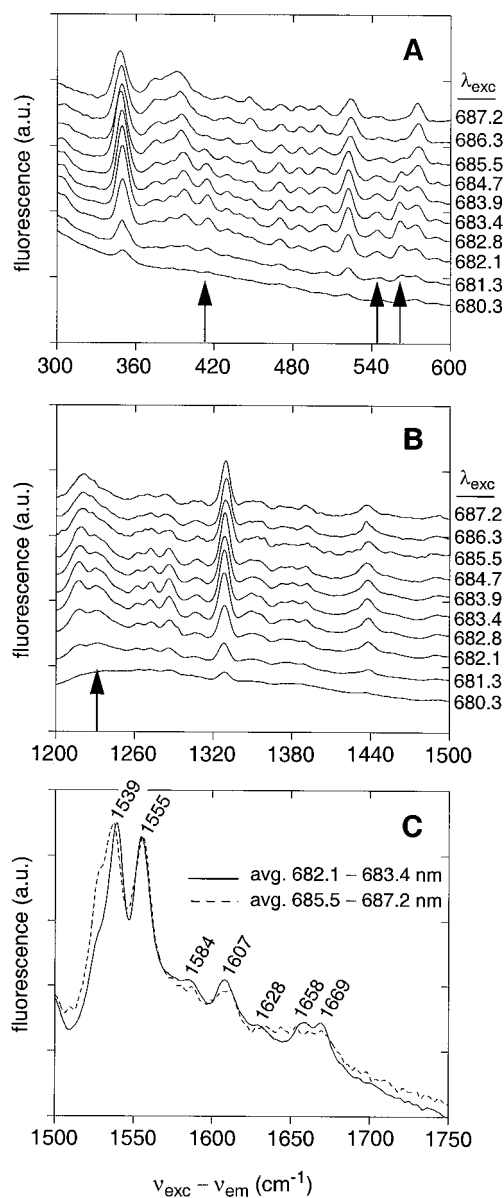


FIGURE 5 (A) Selectively excited emission spectra of CP43 at 5 K, plotted as the difference with the excitation wavenumber between 300 and 600 cm^{-1} . The arrows indicate emission bands that are observable with excitation between 682.1 and 684.7 nm but not observable with excitation between 685.5 and 687.2 nm. (B) As in A, but detected between 1200 and 1500 cm^{-1} . (C) Averages of line-narrowed spectra excited at 5 K at 682.1, 682.8, and 683.4 nm (solid line) and at 685.5, 686.3, and 687.2 nm (dashed line), detected between 1500 and 1750 cm^{-1} .

conversion), but also to a metastable triplet state via inter-system crossing. Preliminary experiments have revealed that at 4 K $\sim 50\%$ of the triplet states are transferred to β -carotene, of which the triplet state had a lifetime of 18 μs (data not shown). The decay of the remaining chlorophyll triplet states showed a major component with a lifetime of $\sim 0.6 \text{ ms}$ and a maximum bleaching at 683 nm and a minor component with a lifetime of 2.7 ms and a maximum bleaching at 684 nm (data not shown). These characteristics are very similar to those observed for the isolated CP47

protein (Groot et al., 1995) and are not explored in more detail in this work.

In a triplet-minus-singlet (T-S) absorbance-difference spectrum one expects to find contributions from 1) an absorption decrease caused by the depopulation of the ground state, 2) a very broad and featureless absorption increase caused by the population of the triplet state, and, possibly, 3) absorbance changes of pigments other than the one on which the triplet is located. The latter contributions may occur if the triplet state is localized on a chlorophyll involved in exciton interaction, because of which the absorption of the original exciton manifold will be replaced by the absorption of a single chlorophyll (in case of an exciton-coupled dimer), or by a new exciton manifold with different properties (in case of a multimer).

Fig. 6 shows T-S spectra detected at 77 K with 12

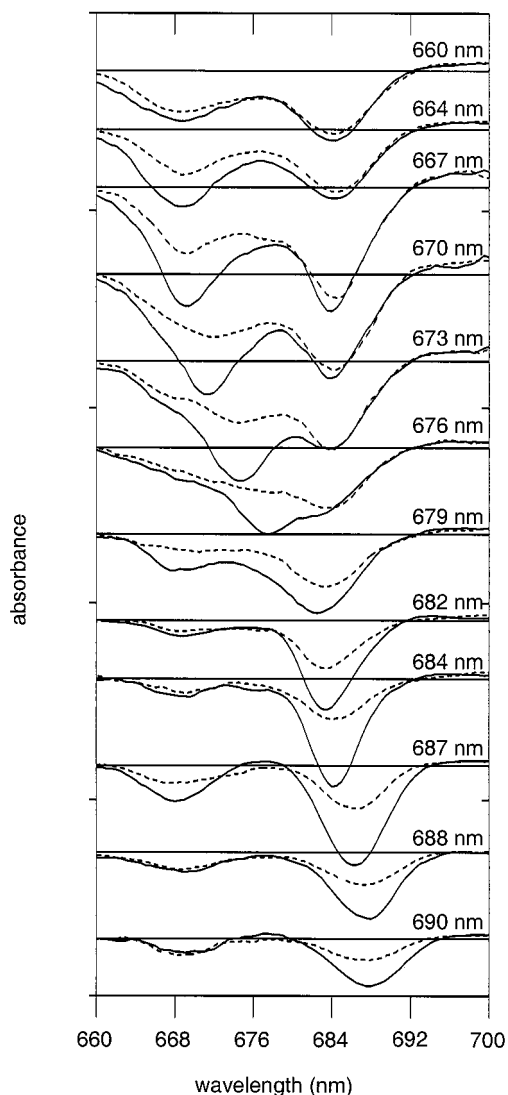


FIGURE 6 Polarized triplet-minus-singlet absorbance-difference spectra, selectively excited at 5 K at 12 different wavelengths between 660 and 690 nm and recorded with parallel or perpendicular polarizers (*solid and dashed lines*, respectively).

excitation wavelengths between 660 and 690 nm and with parallel or perpendicular polarization with respect to the excitation laser (*solid and dashed lines*, respectively). We note that phonon side bands and vibronic lineshapes cannot be resolved in these spectra because the thermal energy at 77 K destroys the line narrowing and because the detection bandwidth (3 nm) is too large for the narrow bands to be observed. The results indicate that upon blue and red excitation ($\lambda_{\text{exc}} \leq 667$ nm, $\lambda_{\text{exc}} \geq 679$ nm) the spectra consist of two bands, while at the intermediate excitation wavelengths a third band appears between the other two (Fig. 6).

The red-most band shows maximum bleaching at 684 nm for $\lambda_{\text{exc}} \leq 673$ nm, a blue shift of this band for $\lambda_{\text{exc}} = 679$ and 682 nm, and a red shift for $\lambda_{\text{exc}} \geq 684$ nm. This band is highly anisotropic upon direct excitation at $\lambda_{\text{exc}} \geq 682$ nm but almost isotropic at $\lambda_{\text{exc}} \leq 676$ nm (see the difference between the *solid and dashed lines* in Fig. 6). The blue-most band shows a maximum bleaching at 668 nm, which apparently does not depend very much on the excitation wavelength. Furthermore this band shows high anisotropy upon direct excitation and almost no anisotropy upon excitation at other wavelengths. The third band is only observed with direct excitation at 670, 673, or 676 nm and is highly anisotropic.

The appearance of a second band with different anisotropy upon excitation in a first band is a strong indication that these bands are coupled by excitonic interaction. In the case of blue excitation downhill energy transfer may also contribute to the spectra, but in case of red excitation this is impossible. Thus, the red-excited absorbance-difference spectrum reflects the bleached absorption of an exciton manifold, with main components around 684 and 668 nm. We note that very similar results were observed with site-selected T-S measurements on the PSII RC (Kwa et al., 1994a), and that in this system exciton bands arise that peak at ~ 680 –684 nm and 668 nm. The main difference between the two systems is that the amplitude of the exciton band at 668 nm is considerably larger in CP43 than in the PSII RC.

The appearance of the middle band is somewhat puzzling. This band probably cannot be explained by “trapping” of excitations on a natural 670–676-nm state of CP43 that is more or less decoupled from the 684–668-nm exciton manifold. In this case one would also expect a contribution at 670–676 nm in the 4 K emission spectrum, which is not observed (Fig. 3 A). Artefacts caused by the measuring procedure also seem unlikely, because the same type of experiments on the PSII RC did not cause unpolarized bleachings upon excitation at 670 nm (Kwa et al., 1994a). It cannot be excluded, however, that unconnected chlorophyll contributes to some extent to the signals in Fig. 6. Unconnected chlorophyll probably has an even higher triplet quantum yield than bound chlorophyll (in view of the $\sim 50\%$ probability of triplet transfer to β -carotene in the CP43 complex) and can sometimes appear during sample storage (see, e.g., Den Hartog et al., 1998). There is an indication, however, that part of the 676-nm absorption belongs to the 684–668-nm manifold, because the anisotropy in the red

tail of the spectrum is negative, suggesting a larger angle between the 676- and 684-nm dipoles than the magic angle of 55° . If only unconnected chlorophyll absorbs at 676 nm, a negative anisotropy is not expected. The CD spectrum seems to confirm the view that around 676 nm exciton states contribute to the spectrum (see below).

It is likely that bands 1 and 2 of the deconvoluted absorption spectrum (Fig. 2 C) both contribute to the T-S spectrum, which would be in agreement with the emission properties (Fig. 3 B). Although the spectral width of the instrument and the applied temperature of 77 K cause some broadening (Table 1), it is clear that the bleaching with $\lambda_{\text{exc}} = 682$ nm, where the narrow band 1 is excited to a large extent, is much narrower than the bleaching with $\lambda_{\text{exc}} = 687$ nm, where only the much broader band 2 is excited (Fig. 6). Another difference between 682–684-nm excitation on the one hand and 687–690-nm excitation on the other is the amplitude of the 668-nm high-exciton band, which seems less pronounced upon 682–684-nm excitation. Because in the latter wavelength region bands 1 and 2 are both excited, it is possible that only band 2 gives rise to a detectable high-exciton band at 668 nm.

We conclude from these experiments that at least bands absorbing near 684 and 668 nm are part of an exciton manifold. We cannot exclude, however, the possibility that more bands take part in this manifold. The T-S spectrum does not give conclusive evidence for the occurrence of additional exciton bands, particularly in the region between the blue- and red-most bands, because the disappearance of exciton states may be compensated for by the appearance of new exciton states, which, in view of the absence of at least one of the partners involved in the original exciton manifold, are expected to be less strongly coupled and thus to absorb in the intermediate part of the spectrum.

Circular dichroism

More information on the possible existence of excitonic interactions in CP43 may be obtained by analysis of circular dichroism (CD) spectra. Fig. 7 shows CD spectra of the purified CP43 complex recorded at 77 and 293 K in the red part of the spectrum. The room temperature spectrum (*dashed line*) has a relatively simple shape with main negative and positive bands peaking at 685.5 and 668 nm, respectively. The 77 K spectrum reveals more fine structure with negative bands at 684, 675, and 660 nm; positive bands at 679.5 and 666.5 nm; and a positive shoulder at 670 nm. The shapes of the spectra differ very much from those of other PSII complexes. For instance, the CP47, PSII RC, and CP26 complexes all give rise to very different fine structures (Kwa et al., 1994b; Otte et al., 1992; van Amerongen et al., 1994) with a negative band at 679–680 nm in all three cases.

It is possible that part of the intense CD signal around 682 nm, in particular the negative band at 684 nm, is caused by the very narrow band 1. The width of band 1 at 77 K should

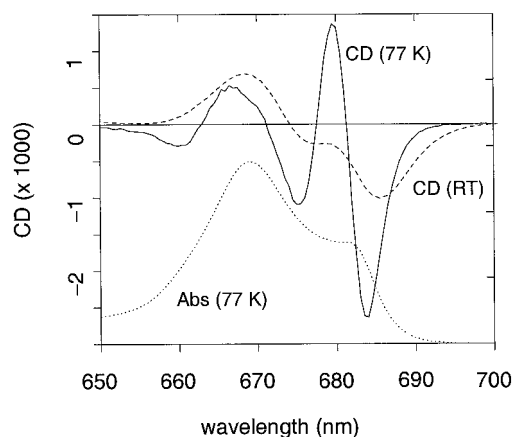


FIGURE 7 Circular dichroism spectra of CP43 between 650 and 700 nm, recorded at room temperature (*dashed line*) or at 77 K (*solid line*). For comparison, the 77 K absorption spectrum is shown as well (*dotted line*).

be ~ 3.3 nm according to the fit presented in Table 1, which is very similar to the width of the negative band at 684 nm. Some broadening could have occurred because of the spectral resolution of the CD measurements (compare the absorption spectra in Figs. 2 and 7), but on the other hand CD bands are usually slightly narrower than absorption bands (Somsen et al., 1996). We note that an involvement of an absorption band in the CD spectrum does not necessarily mean that the pigment causing this absorption band is excitonically coupled. An analysis of the CD spectrum of LH2 complexes from photosynthetic purple bacteria (Koolhaas et al., 1997) has revealed that pigments at opposite sides of the ring, which are too far apart to exhibit significant excitonic interactions, nevertheless give large contributions to the CD signal.

Linear dichroism

We also recorded linear dichroism (LD) spectra of our CP43 preparation. It appeared not to be possible to record LD signals of CP43 by the commonly applied method using a stretched polyacrylamide gel (see, e.g., Hemelrijk et al., 1992), because the protein appeared to denature completely in this type of gel. However, with a stretched gelatin gel (Otte et al., 1992) denaturation did not occur to a significant extent (the *dashed line* in Fig. 8 shows a “normal” 77 K absorption spectrum of CP43 in a gelatin gel), and pronounced LD signals could be recorded (Fig. 8, *full line*). The spectrum shows a positive LD peak at 672.5 nm, clear positive shoulders near 682 and 661 nm, and broad negative peaks centered at 632 and 586 nm. The latter peaks are caused by Q_x transitions of Chl *a* (see, e.g., Kwa et al., 1994b). The shape of our LD spectrum is very similar to the one reported by Breton and Katoh (1987) for a cyanobacterial CP43 complex.

In the case of disc-shaped particles and two-dimensional squeezing, a positive LD implies a larger angle between the transition dipole and the normal of the disc than the magic

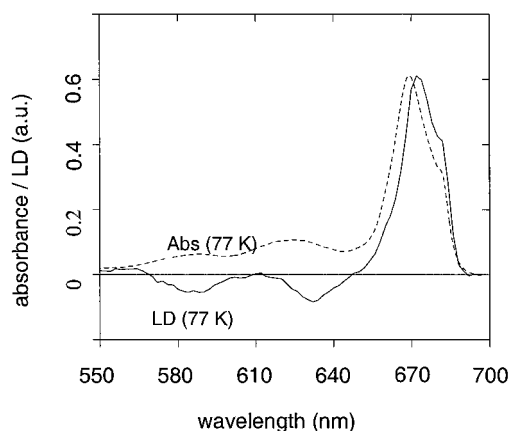


FIGURE 8 Linear dichroism spectrum of CP43 at 77 K (solid line), oriented in a two-dimensionally squeezed gelatin gel. Also shown is the simultaneously recorded absorption spectrum at 77 K (dashed line). The bandwidth of detection was 3 nm for both spectra.

angle, whereas a negative LD implies a shorter angle than the magic angle (van Amerongen et al., 1988). Because for most membrane-bound complexes the plane of the disc equals the plane of the particle in the membrane, positive and negative LD means a small and large angle, respectively, between the transition dipole and the plane of the membrane. Because the average LD at 660–685 nm is positive, the average Q_y transitions of Chl *a* make small angles with the plane of the membrane. Similarly, the negative LD around 632 and 586 nm indicates that the average Q_x transitions of Chl *a* make large angles with the plane of the membrane. The first structural data on the related CP47 complex also suggest a perpendicular orientation of most chlorophylls (Rhee et al., 1998).

In the Q_y absorption region it appears that the transitions at 682 and 661 nm are more pronounced in the LD spectrum than in the absorption spectrum, suggesting that these transitions are more in the plane of the membrane than most other transitions. The broad band at 679 nm seems to cause a smaller LD, based on the steep slope of the red edge of the LD spectrum. Also the band at 669 nm must cause a relatively small LD, in view of the less pronounced LD at the blue edge of the Q_y absorption band. These results do not contradict their assignment as exciton bands (see above), but only indicate that both should make intermediate angles with the plane of the membrane.

Stark spectroscopy

The response of absorption properties to an externally applied electric field is generally known as the Stark effect. Fig. 9 shows the Stark spectrum of CP43 at 77 K (bottom) together with the simultaneously recorded absorption spectrum (top). The Stark spectrum has a very distinct shape and is characterized by positive signals near 684 and 675 nm

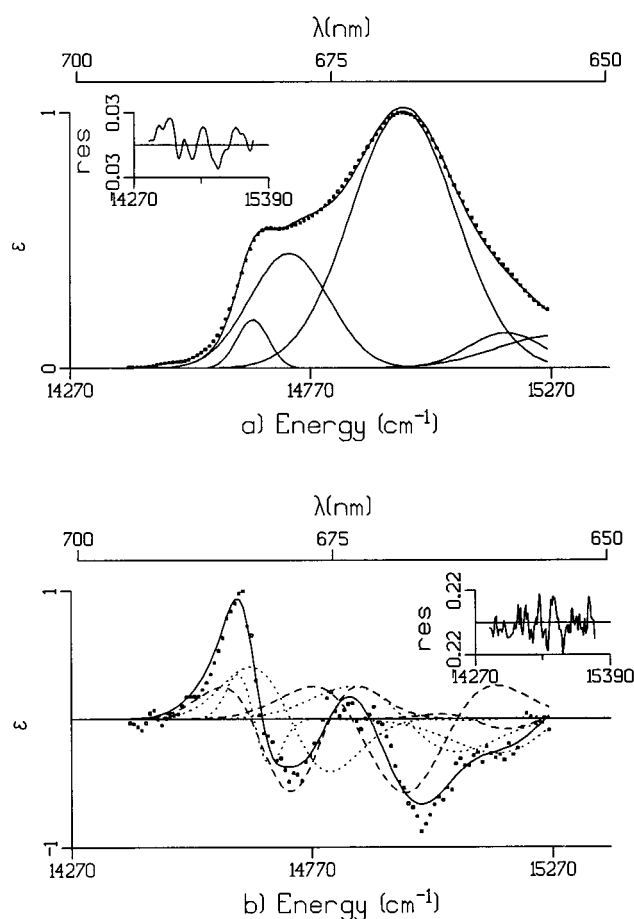


FIGURE 9 Simultaneous fit of 77 K Q_y absorption (top) and Stark spectra (bottom) of CP43 with five independent Gaussian functions for the absorption spectrum (top) and the first and second derivative of these functions for the Stark spectrum (bottom). Data points are indicated by squares, the five Gaussian functions by solid lines, the first derivative contributions of these Gaussians by dotted lines, and second derivative contributions of these Gaussians by dashed lines. The insets show the residuals from the fits of the absorption and Stark spectra.

and by negative signals near 679, 666, and 660 nm. The overall appearance of this spectrum resembles the first derivative of the absorption spectrum (not shown), which even without further data analysis suggests that the difference in polarizability ($\Delta\alpha$) is more important for the Stark spectrum than the difference in permanent dipole moment ($\Delta\mu$). The most remarkable feature of the Stark spectrum of CP43 is its overall size, which is the smallest reported to date of any photosynthetic complex and which is even smaller than that of monomeric Chl *a*.

The simultaneous fitting of the 77 K Stark and absorption spectra resulted in the necessity of five Gaussian bands, the peak positions of which were within 1 nm of those found in Fig. 2 C. The resulting $\Delta\mu$ and $\text{Tr}(\Delta\alpha)$ values of the various bands are listed in Table 2. The $\Delta\mu$ values vary between 0 and 0.3 D f^{-1} and are lower than the 0.9–1.0 D f^{-1} reported for monomeric Chl *a* with either one or two axial ligands (Krawczyk, 1991). The $\text{Tr}(\Delta\alpha)$ values vary between 5 and 6 $\text{\AA}^3 f^{-2}$ and are higher than for monomeric Chl *a*, which

TABLE 2 Values of the difference in permanent dipole moment ($\Delta\mu$) and difference in polarizability ($\text{Tr}(\Delta\alpha)$), obtained from the simultaneous fit of absorption and Stark spectra of CP43 at 77 K

Peak wavelength (nm)	$\Delta\mu$ (D f^{-1})	$\text{Tr}(\Delta\alpha)$ ($\text{\AA}^3 \text{f}^{-2}$)
683	0	5
680	0.3	6
668	0.3	6
659	—	—
655	—	—

See also Fig. 9.

was reported to be 1.5 or 4 $\text{\AA}^3 \text{f}^{-2}$ for Chl *a* with one or two axial ligands, respectively (Krawczyk, 1991). Both the $\Delta\mu$ and $\text{Tr}(\Delta\alpha)$ values of CP43 are significantly smaller than observed for dimeric Chl *a*, for which a $\text{Tr}\Delta\alpha$ of 90 $\text{\AA}^3 \text{f}^{-2}$ and a $\Delta\mu$ of 5 D f^{-1} was reported (Krawczyk, 1991).

In principle, Stark parameters of excitonically coupled pigments can differ very significantly from those of isolated pigments. In the case of the bacterial light-harvesting antenna LH2 (Beekman et al., 1997a) and the special pair of the bacterial reaction center (Middendorf et al., 1993), relatively high values were found for both $\Delta\mu$ (3–7 D f^{-1}) and $\text{Tr}\Delta\alpha$ (500–1500 $\text{\AA}^3 \text{f}^{-2}$). It has recently been shown that these high values cannot be explained with exciton theory only (Somsen et al., 1998). A mixing of charge transfer (CT) states into the excited (excitonic) state by the external electric field can lead to high $\Delta\alpha$ values. High $\Delta\mu$ values can arise from the internal electric field generated by the protein, which transforms the difference polarizability into a difference dipole moment when a Stark experiment is performed (Middendorf et al., 1993). On the other hand, very small $\Delta\mu$ values are expected when the pigments have strongly contrasting orientations, even in the case of considerable orbital overlap, as has been shown for chlorosomes (Frese et al., 1997), which have zero $\Delta\mu$. The $\text{Tr}\Delta\alpha$ values for this system, however, are very high (1700 $\text{\AA}^3 \text{f}^{-2}$), indicating a very significant CT character.

Stark measurements on (sub)complexes of PSII from plants have rarely been performed. The light-harvesting Chl *a/b* protein complexes LHCII and CP29 show $\Delta\mu$ and $\text{Tr}\Delta\alpha$ values for the various subbands that are equal to or slightly higher than the values of monomeric Chl *a* (Krawczyk et al., 1993; C. C. Gradinaru et al., unpublished observations). These findings indicate that excitonic interactions do not determine the spectroscopy of these complexes to a large extent.

The Stark spectroscopy of CP43 as reported here indicates values for $\Delta\mu$ and $\text{Tr}\Delta\alpha$ that differ considerably from those observed in free Chl *a* and the above-mentioned Chl *a/b* complexes. In the following, we will show that these changed Stark parameters can be explained by excitonic coupling. In general, the wavefunction Ψ_k of a system of weakly excitonic coupled pigments can be described as a linear combination of product wavefunctions, each describ-

ing a state where one pigment is in the excited state:

$$\psi_k = \sum_i C_{ki} \cdot \Lambda_i \quad (1)$$

in which Λ_i is the product of the eigenfunctions of the excited state of one molecule with all others in the ground-state and C_{ki} denotes the relative contribution of that state to the exciton state. The change in dipole moment for the *k* exciton state is expressed in the monomer dipole moment change given by

$$\overline{\Delta\mu}_k = \sum_i C_{ki}^2 \cdot \overline{\Delta\mu}_i \quad (2)$$

where $\Delta\mu_k$ and $\Delta\mu_i$ are the permanent difference dipole moments of the exciton states *k* and the monomeric states *i*, respectively.

Because $\sum_i C_{ki} = 1$, it follows that exciton states can have smaller $\Delta\mu$ values than the monomeric pigments of which they are composed, as soon as the pigments are differently oriented. The Stark measurement shows that indeed the CP43 complex is giving rise to excitonic spectra and that the pigments should be oriented strongly antiparallel. To our knowledge these measurements are the first to show this clear excitonic effect on the Stark spectrum.

CONCLUDING REMARKS

Our data indicate that the spectroscopic properties of CP43 are caused by at least three groups of pigments. The first gives rise to the very narrow absorption band, which peaks at 682.5 nm at 5 K and dominates the 5 K emission spectrum. Its total intensity is certainly not more than that of a single chlorophyll, its vibrational fine structure suggests the presence of one axial protein ligand and hydrogen bonding of the $13^1 \text{C}=\text{O}$ group, and its LD suggests that the Q_y transition is at small angles with the plane of the membrane. The T-S data did not reveal a very clear high-exciton band for this chromophore, which, coupled with the small oscillator strength, suggests that it is caused by a single chlorophyll not more than very weakly excitonically coupled to other CP43 chlorophylls. Its relatively long absorption wavelength must therefore originate from specific pigment-protein interactions, while its narrow bandwidth may be caused by a very well-defined binding pocket.

The second group of pigments gives rise to the much broader absorption band peaking around 680 nm. The 4 K absorption at wavelengths longer than 685 nm and the tail at 685–688 nm in the 4 K emission spectrum originate almost exclusively from this group of chlorophylls, while the vibrational fine structure suggests that a mix of 5- and 6-coordinated chlorophylls contributes to this absorption band. The T-S data indicate that this absorption band is coupled with a band at 668 nm with a different orientation, which strongly suggests excitonic coupling. The Stark data reveal an unusually small spectrum, which we attribute to opposing orientations of the monomer dipole moments of the

excitonically coupled pigments and to the virtual absence of charge transfer character of the electronically excited states. The total oscillator strength of band 2 and of the coupled transitions at 668 nm is $\sim 25\text{--}35\%$ of the total absorption in the Q_y region, which suggests that at least three to five chlorophylls contribute to this excitonically coupled system. This number must be regarded as a lower limit, because potential additional exciton bands at intermediate wavelengths may not be observed in the T-S spectrum because of the absorption of the set of pigments on which the triplet is not located.

Finally, there may be a group of pigments absorbing around 670 nm that are not significantly involved in excitonic interactions. It is impossible, however, to estimate how many chlorophylls belong to this group. The fits of the 4 K absorption spectrum indicate that about two-thirds of the absorption is caused by 669-nm transitions, but an unknown part of this absorption is caused by high-exciton components of band 2.

At this point it is worthwhile to compare the spectroscopic properties of CP43 with those of CP47. The proteins are sequence related, bind about the same number of chlorophylls, and have similar organizations with three pairs of transmembrane α -helices as their most conspicuous features (Hankamer et al., 1999). There are small differences in the room temperature absorption spectra (the average chlorophyll $Q_{y,0-0}$ transition peaks at ~ 675 nm in CP47 and at 670 nm in CP43), but this is probably not very relevant for the flow of excitation energy to the reaction center. The thermal energy kT equals 205 cm^{-1} at room temperature, which corresponds to almost 10 nm at 675 nm and which is considerably more than the average energetic difference between the CP47 and CP43 chlorophylls. There are certainly structural differences. The CP47 protein is located in the central part of the PSII-LHCII supercomplex and thus seems to play a role in the dimerization of the PSII core complex, whereas CP43 has a more peripheral location and seems more important for the transfer of excitation energy from the peripheral antenna to the reaction center, simply because it has more contacts with the peripheral antenna than CP47 (see, e.g., Boekema et al., 1999).

The most important spectroscopic differences are formed by the sharp 682-nm band in CP43 (absent in CP47) and the red-shifted 690-nm band in CP47 (absent in CP43). The latter band is responsible for the well-known F-695 fluorescence band at 77 K (see, e.g., Dekker et al., 1995) and probably originates, just like band 1 of CP43, from a single chlorophyll molecule (Van Dorssen et al., 1987b). It is not very likely, however, that the 682-nm chlorophyll in CP43 and the 690-nm chlorophyll in CP47 are bound to corresponding or sequence-related sites, because their orientations are significantly different; the Q_y transition of the 690-nm chlorophyll of CP47 has a perpendicular organization with respect to the plane of the membrane (Van Dorssen et al., 1987a), whereas the Q_y transition of the 682-nm chlorophyll of CP43 has a parallel orientation. Apart from these differences, the spectroscopic properties of CP47 and

CP43 are comparable (the absorption, LD, and CD properties of the two complexes are very similar if the above-mentioned unique features are ignored), which is not unexpected, given the similar organization of most of the chlorophylls in the two complexes (Hankamer et al., 1999).

We finally remark that a relatively "monomeric" red transition, such as that of the narrow 682-nm absorption band of CP43, is not unprecedented. Exciton calculations on Fenna-Matthews-Olson (FMO) complexes from *Prosthechloris aestuarii* and *Chlorobium tepidum* have indicated that the red-most transition is almost exclusively localized on a single bacteriochlorophyll molecule, and that pigment-protein interactions must have caused the red shift of this chromophore (Louwe et al., 1997; Vulto et al., 1998).

We thank Henny van Roon for expert technical assistance and Dr. Herbert van Amerongen for stimulating discussions.

This work was supported by the Netherlands Foundation for Scientific Research (NWO) via the Foundation for Physical Research (FOM) and the Foundation for Life and Earth Sciences (ALW).

REFERENCES

- Alfonso, M., G. Montoya, R. Cases, R. Rodriguez, and R. Picorel. 1994. Core antenna complexes, CP43 and CP47, of higher plant photosystem II. Spectral properties, pigment stoichiometry, and amino acid composition. *Biochemistry*. 33:10494–10500.
- Beekman, L. M. P., R. N. Frese, G. J. S. Fowler, R. Picorel, R. J. Cogdell, I. H. M. van Stokkum, C. N. Hunter, and R. van Grondelle. 1997a. Characterization of the light harvesting antennas of photosynthetic purple bacteria by Stark spectroscopy. 2. LH2 complexes: influence of the protein environment. *J. Phys. Chem. B*. 101:7293–7301.
- Beekman, L. M. P., M. Steffen, I. H. M. van Stokkum, J. D. Olsen, C. N. Hunter, S. G. Boxer, and R. van Grondelle. 1997b. Characterization of the light-harvesting antennas of photosynthetic purple bacteria by Stark spectroscopy. 1. LH1 antenna complex and the B820 subunit from *Rhodospirillum rubrum*. *J. Phys. Chem. B*. 101:7284–7292.
- Boekema, E. J., B. Hankamer, D. Bald, J. Kruij, J. Nield, A. F. Boonstra, J. Barber, and M. Rögner. 1995. Supramolecular structure of the photosystem II complex from green plants and cyanobacteria. *Proc. Natl. Acad. Sci. USA*. 92:175–179.
- Boekema, E. J., H. van Roon, F. Calkoen, R. Bassi, and J. P. Dekker. 1999. Multiple types of association of photosystem II and its light-harvesting antenna in partially solubilized photosystem II membranes. *Biochemistry*. 38:2233–2239.
- Boekema, E. J., H. van Roon, and J. P. Dekker. 1998. Specific association of photosystem II and light-harvesting complex II in partially solubilized photosystem II membranes. *FEBS Lett*. 424:95–99.
- Boxer, S. G. 1996. Stark spectroscopy of photosynthetic systems. In *Biophysical Techniques*. J. Ames and A. J. Hoff, editors. Kluwer Academic Publishers, Dordrecht, The Netherlands. 177–189.
- Breton, J., and S. Katoh. 1987. Orientation of the pigments in photosystem II: low temperature linear-dichroism study of a core particle and of its chlorophyll-protein subunits isolated from *Synechococcus sp.* *Biochim. Biophys. Acta*. 892:99–107.
- Carbonera, D., G. Giacometti, G. Agostini, A. Angerhofer, and V. Aust. 1992. ODMR of carotenoid and chlorophyll triplets in CP43 and CP47 complexes of spinach. *Chem. Phys. Lett*. 194:275–281.
- Dekker, J. P., N. R. Bowlby, and C. F. Yocum. 1989. Chlorophyll and cytochrome *b*-559 content of the photochemical reaction center of photosystem II. *FEBS Lett*. 254:150–154.
- Dekker, J. P., A. Hassoldt, Å. Pettersson, H. van Roon, M.-L. Groot, and R. van Grondelle. 1995. On the nature of the F695 and F685 emission of photosystem II. In *Photosynthesis: From Light to Biosphere*, Vol. 1 P.

- Mathis, editor. Kluwer Academic Publishers, Dordrecht, the Netherlands. 53–56.
- Den Hartog, F. T. H., F. Vacha, A. J. Lock, J. Barber, J. P. Dekker, and S. Völker. 1998. Comparison of the excited-state dynamics of five- and six-chlorophyll photosystem II reaction center complexes. *J. Phys. Chem. B.* 102:9174–9180.
- Eijkelhoff, C., J. P. Dekker, and E. J. Boekema. 1997. Characterization by electron microscopy of dimeric photosystem II core complexes from spinach with and without CP43. *Biochim. Biophys. Acta.* 1321:10–20.
- Eijkelhoff, C., H. van Roon, M.-L. Groot, R. van Grondelle, and J. P. Dekker. 1996. Purification and spectroscopic characterization of photosystem II reaction center complexes isolated with or without Triton X-100. *Biochemistry.* 35:12864–12872.
- Frese, R. N., U. Oberheide, I. H. M. van Stokkum, R. van Grondelle, M. Foidl, J. Oelze, and H. van Amerongen. 1997. The organization of bacteriochlorophyll *c* in chlorosomes from *Chloroflexus aurantiacus* and the structural role of carotenoids and protein. An absorption, linear dichroism, circular dichroism and Stark spectroscopy study. *Photosynth. Res.* 54:115–126.
- Fujiwara, M., and M. Tasumi. 1986a. Resonance Raman and infrared studies on axial coordination to chlorophylls *a* and *b* in vitro. *J. Phys. Chem.* 90:250–255.
- Fujiwara, M., and M. Tasumi. 1986b. Metal-sensitive bands in the Raman and infrared spectra of intact and metal-substituted chlorophyll *a*. *J. Phys. Chem.* 90:5646–5650.
- Ghanotakis, D. F., D. M. Demetriou, and C. F. Yocum. 1987. Isolation and characterization of an oxygen-evolving photosystem II reaction center core preparation and a 28 kDa Chl-*a*-binding protein. *Biochim. Biophys. Acta.* 891:15–21.
- Groot, M.-L., E. J. G. Peterman, P. J. M. van Kan, I. H. M. van Stokkum, J. P. Dekker, and R. van Grondelle. 1994. Temperature dependent triplet and fluorescence quantum yields of the photosystem II reaction center described in a thermodynamic model. *Biophys. J.* 67:318–330.
- Groot, M.-L., E. J. G. Peterman, I. H. M. van Stokkum, J. P. Dekker, and R. van Grondelle. 1995. Triplet and fluorescing states of the CP47 antenna complex of photosystem II studied as a function of temperature. *Biophys. J.* 68:281–290.
- Hankamer, B., J. Barber, and E. J. Boekema. 1997. Structure and membrane organization of photosystem II from green plants. *Annu. Rev. Plant Phys. Plant Mol. Biol.* 48:641–672.
- Hankamer, B., E. P. Morris, and J. Barber. 1999. Revealing the structure of the oxygen-evolving core dimer of photosystem II by cryoelectron crystallography. *Nature Struct. Biol.* 6:560–564.
- Hasler, L., D. Ghanotakis, B. Fedtke, A. Spyridaki, M. Miller, S. A. Mueller, A. Engel, and G. Tsiotis. 1997. Structural analysis of photosystem II: comparative study of cyanobacterial and higher plant photosystem II complexes. *J. Struct. Biol.* 119:273–283.
- Hemelrijk, P. W., S. L. S. Kwa, R. van Grondelle, and J. P. Dekker. 1992. Spectroscopic properties of LHC-II, the main light-harvesting chlorophyll *a/b* protein complex from chloroplast membranes. *Biochim. Biophys. Acta.* 1098:159–166.
- Koolhaas, M. H. C., G. van der Zwan, R. N. Frese, and R. van Grondelle. 1997. Red shift of the zero crossing in the CD spectra of the LH2 antenna complex of *Rhodospseudomonas acidophila*: a structure-based study. *J. Phys. Chem. B.* 101:7262–7270.
- Krawczyk, S. 1991. Electrochromism of chlorophyll *a* monomer and special pair dimer. *Biochim. Biophys. Acta.* 1056:64–70.
- Krawczyk, S., Z. Krupa, and W. Maksymiec. 1993. Stark spectra of chlorophylls and carotenoids in antenna pigment-proteins LHC-II and CP-II. *Biochim. Biophys. Acta.* 1143:273–281.
- Kwa, S. L. S., F. G. Groenewald, J. P. Dekker, R. van Grondelle, H. van Amerongen, S. Lin, and W. S. Struve. 1992. Steady-state and time-resolved polarized light spectroscopy of the green plant light-harvesting complex II. *Biochim. Biophys. Acta.* 1101:143–146.
- Kwa, S. L. S., C. Eijkelhoff, R. van Grondelle, and J. P. Dekker. 1994a. Site-selection spectroscopy of the reaction center complex of photosystem II. I. Triplet-minus-singlet absorption difference: a search for a second exciton band of P-680. *J. Phys. Chem.* 98:7702–7711.
- Kwa, S. L. S., S. Völker, N. T. Tilly, R. van Grondelle, and J. P. Dekker. 1994b. Polarized site-selection spectroscopy of chlorophyll *a* in detergent. *Photochem. Photobiol.* 59:219–228.
- Liptay, W. 1974. Dipole moments and polarizabilities of molecules in excited electronic states. In *Excited States*, Vol. 1. C. E. Lim, editor. Academic Press, New York. 128–190.
- Louwe, R. J. W., J. Vrieze, A. J. Hoff, and T. J. Aartsma. 1997. Towards an integral interpretation of the optical steady-state spectra of the FMO-complex of *Prosthecochloris aestuarii*. 2. Exciton simulations. *J. Phys. Chem. B.* 101:11280–11287.
- Lutz, M., and B. Robert. 1988. Chlorophylls and photosynthetic membrane. In *Biological Application of Raman Spectroscopy*. T. G. Spiro, editor. Wiley, New York. 347–411.
- Middendorf, T. R., L. T. Mazzola, K. Lao, M. A. Steffen, and S. G. Boxer. 1993. Stark effect (electroabsorption) spectroscopy of photosynthetic reaction centers at 1.5 K: evidence that the special pair has a large excited-state polarizability. *Biochim. Biophys. Acta.* 1143:223–234.
- Newell, W. R., H. van Amerongen, J. Barber, and R. van Grondelle. 1991. Spectroscopic characterization of the reaction centre of photosystem II using polarised light: evidence for β -carotene excitons in PS II reaction centres. *Biochim. Biophys. Acta.* 1057:232–238.
- Otte, S. C. M., R. van der Vos, and H. J. van Gorkom. 1992. Steady state spectroscopy at 6 K of the isolated photosystem II reaction centre: analysis of the red absorption band. *J. Photochem. Photobiol. B Biol.* 15:5–14.
- Personov, R. I. 1983. In *Spectroscopy and Excitation Dynamics of Condensed Molecular Systems*. V. M. Agranovich and R. M. Hochstrasser, editors. North-Holland, Amsterdam. 555–619.
- Peterman, E. J. G., T. Pullerits, R. van Grondelle, and H. van Amerongen. 1997. Electron-phonon coupling and vibronic fine structure of light-harvesting complex II of green plants: temperature dependent absorption and high-resolution fluorescence spectroscopy. *J. Phys. Chem. B.* 101:4448–4457.
- Peterman, E. J. G., H. van Amerongen, R. van Grondelle, and J. P. Dekker. 1998a. The nature of the excited state of the reaction center of photosystem II of green plants. A high-resolution fluorescence spectroscopy study. *Proc. Natl. Acad. Sci. USA.* 95:6128–6133.
- Peterman, E. J. G., S.-O. Wenk, T. Pullerits, L.-O. Pålsson, R. van Grondelle, J. P. Dekker, M. Rögner, and H. van Amerongen. 1998b. Fluorescence and absorption spectroscopy of the weakly fluorescing chlorophyll *a* in cytochrome *b_f* of *Synechocystis* PCC 6803. *Biophys. J.* 75:389–398.
- Renge, I., R. van Grondelle, and J. P. Dekker. 1996. Matrix and temperature effects on absorption spectra of β -carotene and pheophytin *a* in solution and in green plant photosystem II. *J. Photochem. Photobiol. A.* 96:109–122.
- Rhee, K.-H., E. P. Morris, J. Barber, and W. Kühlbrandt. 1998. Three-dimensional structure of the plant photosystem II reaction centre at 8 Å resolution. *Nature.* 396:283–286.
- Rhee, K.-H., E. P. Morris, D. Zheleva, B. Hankamer, W. Kühlbrandt, and J. Barber. 1997. Two-dimensional structure of plant photosystem II at 8 Å resolution. *Nature.* 389:522–526.
- Schubert, W.-D., O. Klukas, W. Saenger, H. T. Witt, P. Fromme, and N. Krauss. 1998. A common ancestor for oxygenic and anoxygenic photosynthetic systems: a comparison based on the structural model of photosystem I. *J. Mol. Biol.* 280:297–314.
- Somsen, O. J. G., V. Chernyak, R. N. Frese, R. van Grondelle, and S. Mukamel. 1998. Excitonic interactions and Stark spectroscopy of light-harvesting systems. *J. Phys. Chem. B.* 102:8893–8908.
- Somsen, O. J. G., R. van Grondelle, and H. van Amerongen. 1996. Spectral broadening of interacting pigments: polarized absorption by photosynthetic proteins. *Biophys. J.* 71:1934–1951.
- van Amerongen, H., B. M. van Bolhuis, S. Betts, R. Mei, R. van Grondelle, C. F. Yocum, and J. P. Dekker. 1994. Spectroscopic characterization of CP26, a chlorophyll *a/b* binding protein of the higher plant photosystem II complex. *Biochim. Biophys. Acta.* 1188:227–234.
- van Amerongen, H., H. Vasmel, and R. van Grondelle. 1988. Linear dichroism of chlorosomes from *Chloroflexus aurantiacus* in compressed gels and electric fields. *Biophys. J.* 54:65–76.
- Van Dorssen, R. J., J. Breton, J. J. Plijter, K. Satoh, H. J. van Gorkom, and J. Amesz. 1987a. Spectroscopic properties of the reaction center and of

- the 47 kDa chlorophyll protein of photosystem II. *Biochim. Biophys. Acta.* 893:267–274.
- Van Dorssen, R. J., J. J. Plijter, J. P. Dekker, A. den Ouden, J. Amesz, and H. J. van Gorkom. 1987b. Spectroscopic properties of chloroplast grana membranes and of the core of photosystem II. *Biochim. Biophys. Acta.* 890:134–143.
- Van Leeuwen, P. J. 1993. The redox cycle of the oxygen-evolving complex of photosystem II. Doctoral thesis. University of Leiden, Leiden, the Netherlands.
- Vischers, R. W., M. C. Chang, F. van Mourik, P. S. Parkes-Loach, B. A. Heller, P. A. Loach, and R. van Grondelle. 1991. Fluorescence polarization and low-temperature absorption spectroscopy of a subunit form of light-harvesting complex I from purple photosynthetic bacteria. *Biochemistry.* 30:5734–5742.
- Vulto, S. I. E., M. A. de Baat, R. J. W. Louwe, H. P. Permentier, T. Neef, M. Miller, H. van Amerongen, and T. J. Aartsma. 1998. Exciton simulations of optical spectra of the FMO complex from the green sulfur bacterium *Chlorobium tepidum* at 6 K. *J. Phys. Chem. B.* 102:9577–9582.